Relativistic Coulomb excitation in ^{32}Mg near 200 MeV/nucleon with a thick target

K. Li (李阔昂),[1,2] Y. Ye (叶沿林),[1,*] T. Motobayashi (本林透),[3,†] H. Scheit,[3] P. Doornenbal,[3] S. Takeuchi (武内聪),[3] N. Aoi (青井考),[3] M. Matsushita (松下昌史),[3] E. Takeshita (竹下英里),[3] D. Pang (庞丹阳),[4] and H. Sakurai (櫻井博儀)[3]

[1]*School of Physics and State Key Laboratory of Nuclear Physics and Technology, Peking University, Beijing 100871, China*

[2]*Institute of Modern Physics, Chinese Academy of Sciences, Lanzhou 730000, China*

[3]*RIKEN Nishina Center, Wako, Saitama 351-0198, Japan*

[4]*School of Physics and Nuclear Energy Engineering, Beihang University, Beijing 100191, China*

(Received 4 November 2014; revised manuscript received 3 June 2015; published 7 July 2015)

Intermediate-energy Coulomb excitation of ^{32}Mg using in-beam γ-ray spectroscopy with a relatively thick lead target was studied at a beam energy of 195 MeV/nucleon at the RIKEN Radioactive Isotope Beam Factory (RIBF). The angular distribution of the inelastic scattering was analyzed with distorted-wave calculations taking into account both the Coulomb and the nuclear excitation contributions. A $B(E2)$ value of 432(51) e^2 fm^4 was extracted, which agrees with most of the previously reported results obtained at several tens of MeV/nucleon. Our investigation demonstrates that the electromagnetic properties of exotic nuclei can be studied with Coulomb excitation at beam energies of a few hundreds of MeV/nucleon, where a thicker target can be used to increase the excitation yields.

DOI: 10.1103/PhysRevC.92.014608 PACS number(s): 23.20.−g, 25.60.−t, 25.70.De

I. INTRODUCTION

Coulomb excitation has a long history in the study of nuclear structure especially for the quadrupole collectivity [1–3]. The beam energy is usually set below the Coulomb barrier (several MeV/nucleon) to avoid the nuclear interaction in the excitation process. With the recent development of fragmentation-based radioactive-isotope (RI) beam facilities, intermediate-energy (several tens of MeV/nucleon) Coulomb excitation studied in inverse kinematics has been successfully applied and many results have been obtained [4,5]. In most cases, the Coulomb excitation dominates over the nuclear-interaction component and $B(E2)$ values can be reliably extracted even at these high energies [6–10]. The selection of events at small scattering angles, corresponding to large impact parameters, is sometimes crucial in suppressing the nuclear-interaction contribution. In most experiments, in-flight deexcitation γ rays are measured to specify the energy levels and to tag the corresponding inelastic scattering.

More recently, experiments at several hundreds of MeV/nucleon have been performed [11–14]. An experimental advantage at higher energies is the possibility to employ a thicker target to increase the experimental γ-ray yield. However, the Doppler correction and the suppression of low-energy atomic background become more challenging. In addition, the larger angular straggling in a thicker target impedes a precise measurement of the angular distribution. It causes more ambiguity, in principle, in the impact parameter selection to separate the nuclear contribution. It is evident that all these effects associated with a thick target should be examined to reliably apply Coulomb excitation to nuclear spectroscopy in this higher-energy regime.

Intermediate-energy Coulomb excitation was pioneered in the mid-1990s for the nucleus ^{32}Mg [4] which is located in the so-called "island of inversion" [15]. This nucleus has also been studied afterwards at various laboratories [10,16–18]. The reported results show that ^{32}Mg has a large $B(E2)$ value together with a low first 2^+ energy, indicating the disappearance of the $N = 20$ shell closure. Considering that these measurements were made at energies up to 50 MeV/nucleon, it would be interesting to take this nucleus as a sample to investigate the validity of Coulomb excitation at higher energies for the extraction of $B(E2)$ values. If successful, the method can be applied to more neutron-rich unstable nuclei provided by the BigRIPS fragment separator [19–21] at the RIKEN Radioactive Isotope Beam Factory (RIBF) [22,23] with the advantages related to thick target and high RI-beam intensities.

II. EXPERIMENTAL SETUP

The RIBF is operated by the RIKEN Nishina Center and the Center for Nuclear Study, University of Tokyo. A primary beam of ^{48}Ca at 345 MeV/nucleon with an intensity of 2 pnA bombarded a 15-mm-thick beryllium production target. Projectile fragmentation products were analyzed and separated using the magnet rigidity, $B\rho$, with an aluminum wedge inserted at the dispersive focus F1 at the first stage of BigRIPS. The second stage of BigRIPS was used to identify the fragments with the ΔE-$B\rho$-TOF (time of flight) method, where the energy loss ΔE was measured by an ionization chamber installed at the focus F7, $B\rho$ was determined from the position measurement by parallel plate avalanche counters (PPACs) [24] at the dispersive focus F5, and the TOF was measured between two plastic scintillators installed at F3 and F7 with a flight length of 47 m.

After the selection and identification, the secondary beam of ^{32}Mg was transported to the F8 focus with an intensity of about 10^3 particle/s at ∼213 MeV/nucleon, a purity of ∼45%, and was incident on a 3.37 g/cm^2 lead target (reaction target). We note that this target thickness was several times larger than that usually used at energies at around 50 MeV/nucleon. At

*yeyl@pku.edu.cn
†motobaya@riken.jp

the center of the lead target, the energy of ^{32}Mg was about 195 MeV/nucleon, while the total energy loss in the target was ∼17%.

The target, set in a vacuum chamber, was surrounded by DALI2 (Detector Array for Low-Intensity radiation 2) [25], which consisted of 177 NaI(Tl) scintillators covering laboratory angles from 11° to 170°. A 1-mm-thick lead shield was inserted between the target chamber and detectors to absorb low-energy photons originating from atomic processes during the collision. DALI2 had an energy resolution of about 6% [full width at half maximum (FWHM)] and an efficiency of about 13% for the full-energy peak of the 1.33-MeV γ ray emitted from a standard ^{60}Co source, which were well reproduced by a Monte Carlo simulation with the GEANT4 code [26].

The scattering angles of the ^{32}Mg nuclei in the laboratory system were measured by two sets of PPACs installed upstream and downstream of the target. The scattering-angle resolution was estimated to be 11 mrad in the laboratory frame, including both effects of the detector position resolution and the multiple scattering in the reaction target. The overall efficiency of the PPACs installed downstream of the target was as high as 95%.

The products of secondary reactions were analyzed with the ZeroDegree spectrometer (ZDS) [21,27], which had an angular acceptance of 90 × 60 mrad^2. The ΔE-$B\rho$-TOF method was again used for particle identification of the scattered particles, with ΔE measured by an ionization chamber at the final focus F11, $B\rho$ determined from the positions measured by the PPACs located at F10 with an efficiency of 90% for $Z = 12$ particles, and the TOF measured by the two plastic scintillators at F8 and F11 with a flight length of 37 m. The resolutions of Z and A were 0.35 and 0.09 (FWHM), respectively, sufficient to separate ^{32}Mg from other isotopes.

III. RESULTS AND DISCUSSION

Figure 1(a) shows the γ-ray spectrum in the rest frame for the ^{32}Mg + Pb inelastic scattering. A peak at around 885 keV, corresponding to the known $2_1^+ \rightarrow 0_{\text{g.s.}}^+$ transition in ^{32}Mg, is clearly seen, whereas the γ background below the peak is rather high. Figure 2 shows the Doppler-corrected γ-ray energy plotted versus the detector number, which corresponds to the laboratory angles (in reverse order) relative to the beam direction. By the Doppler correction, the low-energy background for the detectors at backward angles is extended to high energies. The peak to background ratio of the spectrum is much improved by limiting the γ-ray emission angle to be smaller than 90°, as shown in Fig. 1(b). According to GEANT4 simulations, the efficiency for the Doppler-corrected ^{32}Mg 2^+ peak is reduced from 17% to 12% under this condition, which is still acceptable for cross-section measurements. A simulation was performed for the 885-keV γ rays from ^{32}Mg moving at a velocity of $\beta = 0.58$ in the laboratory frame. The absorption by the target chamber and the lead shield, the geometry of NaI(Tl) detectors, the energy resolution of each detector, and the lifetime of the first 2^+ state (17.9 ps corresponds to $B(E2) = 432\ e^2\,\text{fm}^4$ obtained in this work) were taken into account. Despite the large velocity spread in the Doppler correction caused by the thick target, the simulation showed that the emission of γ rays takes place mostly after the escape of the ^{32}Mg from the target. Thus, the $\beta = v/c$ value measured event-by-event at the ZeroDegree spectrometer could be used for Doppler corrections. In addition, the angular distribution of the emitted γ rays calculated by the coupled-channel code ECIS97 [28] was used in the simulation, which gave about 10% difference of the efficiency in comparison to

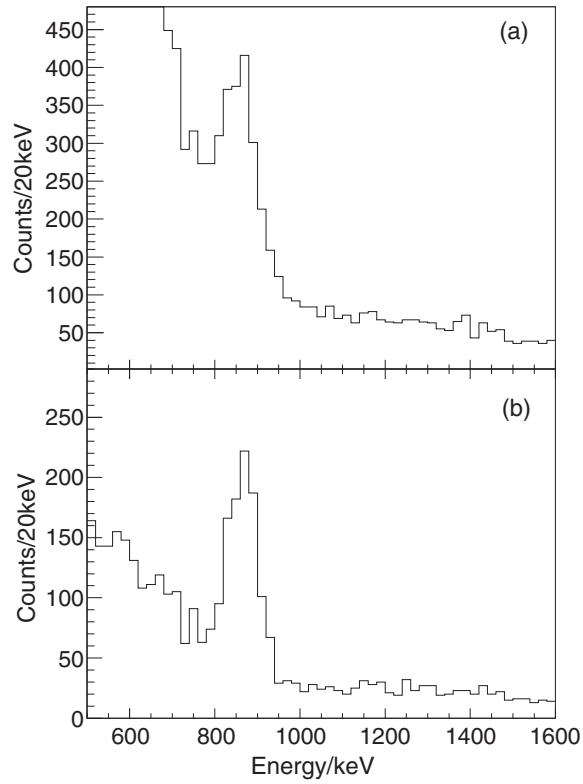

FIG. 1. Doppler-corrected γ-ray spectrum from ^{32}Mg + Pb inelastic scattering constructed with all 177 DALI2 detectors (a) and with only 102 forward-angle detectors (b). The low-energy background is highly suppressed in panel (b).

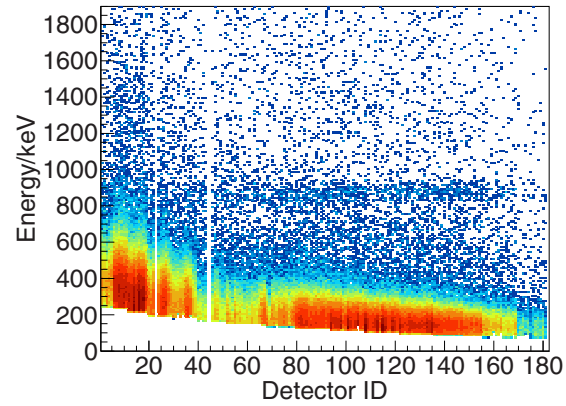

FIG. 2. (Color online) Doppler-corrected γ-ray spectrum from ^{32}Mg inelastic scattering plotted against the detector number. A higher number corresponds to a smaller angle in the laboratory frame. It is evident that the low-energy background is more significant for backward-angle detectors.

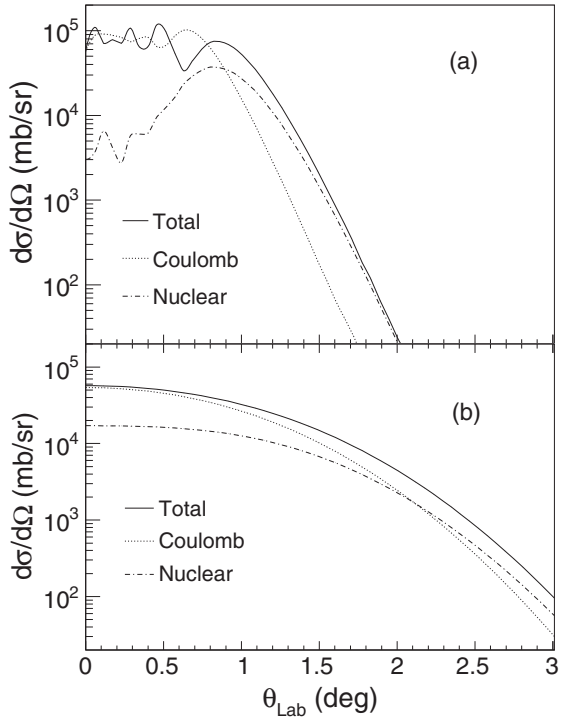

FIG. 3. Contributions from Coulomb and nuclear potentials to the $0^+_{g.s} \rightarrow 2^+_1$ inelastic excitation cross sections, $\beta_{2c} = \beta_{2n} = 0.5$, calculated within the coupled-channel approach. Panel (b) is the same as panel (a) but convoluted with the angular resolution.

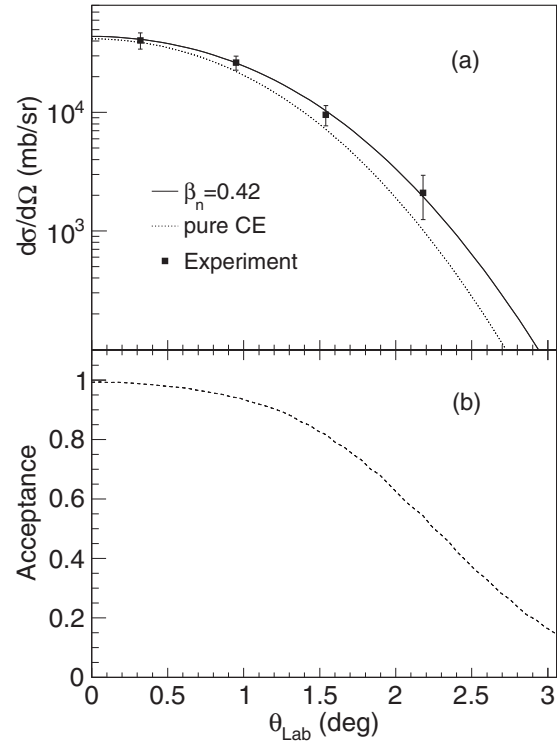

FIG. 4. The experimental differential cross sections for inelastic excitation of the 2^+_1 state in ^{32}Mg are presented by the rectangles in panel (a). The solid line shows the coupled-channel calculation for the corresponding excitation. The curve assuming pure Coulomb excitation is also presented with the dotted line. The angular acceptance of ZDS is shown in panel (b).

an isotropic γ-ray distribution. The resolution and efficiency for the 885-keV γ ray at $v/c = 0.58$ were simulated to be 10% (FWHM) and 11.9%, respectively, when the energy measured in detectors at forward angles ($\theta < 90^\circ$) was used to reconstruct the spectrum.

In Refs. [6,7,9] the differential cross section at a narrow range of the scattering angle was used to minimize contributions from the nuclear interaction in extracting the $B(E2)$ value. However, at the present high beam energy with the thick target, the same method is hard to apply due to the forward focusing of the reaction products and multiple scattering in the target as discussed earlier. Therefore, the entire angular distribution is analyzed in this work. Figure 3 shows the calculated angular distribution, which is the coherent sum of Coulomb and nuclear contributions to the $0^+_{g.s} \rightarrow 2^+_1$ excitation cross section. The distribution is shown without [Fig. 3(a)] and with [Fig. 3(b)] angular smearing by multiple scattering in the same manner as described in Ref. [29]. The calculations were performed using the coupled-channel code ECIS97 based on the rotational model. The deformation parameters were set to be $\beta_{2c} = \beta_{2n} = 0.5$ for both Coulomb and nuclear excitations. Because no optical potential based on experimental data is available for a similar system, we employed a theoretically derived potential called GDM07 [30]. This global potential with both real and imaginary parts is constructed from the nucleon-nucleon effective interaction based on the G-matrix theory (for more details see Ref. [30]). We rely on this potential, which reproduces well various experimental data in a wide range of energies and projectile-target combinations.

One can see from Fig. 3(a) that at small scattering angles of $\theta < 1.0^\circ$ the Coulomb interaction dominates the cross section. Note that the angle 1° corresponds to the impact parameter $b = r_1 + r_2 + 5$ fm (with $r = 1.2A^{1/3}$ fm) if a pure Coulomb trajectory is assumed. As the scattering angle increases, the nuclear force starts to play a major role. By taking into account the angular resolution [Fig. 3(b)], the cross section at $\theta < 1^\circ$ contains the nuclear excitation component of about 20%, indicating the necessity of evaluating nuclear contribution even at these very forward angles as in the case of the first Coulomb excitation study [4].

The ^{32}Mg + Pb experimental angular distribution for the $0^+_{g.s} \rightarrow 2^+_1$ excitation is shown in the top of Fig. 4 together with theoretical predictions. The angular acceptance of ZDS is presented in the bottom figure by the dashed curve. As demonstrated in Fig. 1, no γ-ray line from higher-lying states is visible with statistical significance. However, various higher-lying states with sizable excitation strength were observed in a previous proton inelastic scattering experiment at $E_{in} = 46.5$ MeV/nucleon in inverse kinematics [29]. These higher-lying states should also be excited in the present experiment and therefore are expected to feed the first 2^+ state, requiring some γ-ray yield to be subtracted from the observed 2^+ excitation cross section. This feeding was estimated by distorted-wave (coupled-channel) calculations using the excitation energies and deformation lengths extracted in the proton

inelastic-scattering study tabulated in Ref. [29]. The total yield of the feeding obtained by summing contributions from individual higher states was 11.2(27) mb, which accounted for 14(3)% of the observed $2^+ \rightarrow 0^+$ γ-ray yield. The error includes the uncertainty of the J^π and β values of the higher states. Thus, the experimental yield is scaled down by 14% to extract the 2^+ excitation cross section.

The nuclear deformation for the 2_1^+ state excitation, β_{2n}, was derived to be 0.421(35) using the result obtained in the parallel measurement of proton inelastic scattering at the same incident energy [31], $\beta_{2n} = 0.41(3)$. The probe dependence of the extracted nuclear deformation was evaluated by the method described in Ref. [32] applied to the $^{16}\mathrm{C} + ^{208}\mathrm{Pb}$ inelastic scattering. The solid curve in Fig. 4 represents the best fit with $\beta_c = 0.443(27)$ corresponding to $B(E2) = 432(51)\ e^2\,\mathrm{fm}^4$, which is adopted in the present study. The quoted error includes the systemic error deduced from the uncertainties in the yield of the γ peak (4.5%), the simulation of γ-ray efficiency (10%), the feeding correction (4.1%), and the nuclear deformation (3.5%), which were combined in quadrature. It should be noted that the simple assumption $\beta_{2n} = \beta_{2c}$ leads to $B(E2) = 416(47)\ e^2\,\mathrm{fm}^4$, slightly smaller but in agreement with the value $432(51)\ e^2\,\mathrm{fm}^4$ we adopted within the errors.

As one can see in Fig. 4, the shape of the theoretical angular distribution reproduces well the experimental data, whereas the distribution for the pure Coulomb excitation curve (dotted curve) deviates, indicating that the effect from the nuclear excitation is reasonably accounted for. In this analysis, the nuclear excitation contributes about 18% to the total cross section, which is higher than the case of Sn isotopes excited at the same beam energy region [14]. This should be due to the difference in Z dependence of the relative contributions from the Coulomb and nuclear excitations: larger relative contributions of the nuclear component are expected for lower-Z nuclei as pointed out, for example, in Ref. [33]. Besides, the 18% effect of nuclear contribution is larger than about 3% estimated in Ref. [4] for the lower-energy ($\sim$50 MeV/nucleon) case. These conditions indicate that the nuclear-excitation mechanism should be properly treated to extract the $B(E2)$ values from the Coulomb excitation data in this mass region taken at this energy regime.

In the analysis, the beam energy at the middle of the production target, 195 MeV/nucleon, was used for the distorted-wave calculations. Though the beam lost 36 MeV/nucleon of energy in the target, which corresponds to a 3.5% variation of the predicted cross section, the use of 195 MeV/nucleon as an averaged incident energy leads to a negligible error for the extracted $B(E2)$ value. Another concern for the beam-energy variation is the optical potential, which is expected to significantly vary in the relevant energy region. Indeed at small relative distances the real part of the employed GDM07 potential changes its sign in the incident-energy region around 200 MeV/nucleon. However, as peripheral collisions dominate the $^{32}\mathrm{Mg} + \mathrm{Pb}$ inelastic scattering in this energy domain, the theoretical cross sections are sensitive only to the surface part of the potential, which has a less pronounced energy dependence. Thus, the cross section changes by only 0.9% for the variation of the ^{32}Mg energy in the target.

Our $B(E2)$ value, $432(51)\ e^2\,\mathrm{fm}^4$, agrees with most of the previously reported values obtained from various experiments preformed at lower energy (several tens of MeV/nucleon) at different facilities, such as $454(78)\ e^2\,\mathrm{fm}^4$ [4], $440(55)\ e^2\,\mathrm{fm}^4$ [17], $447(57)\ e^2\,\mathrm{fm}^4$ [10], and $449(53)\ e^2\,\mathrm{fm}^4$ [16]. These numbers are with minor or no feeding-back corrections. Though the effect should be smaller than at 200 MeV/nucleon, these $B(E2)$ values might become slightly smaller if a correction in the same manner as in the present analysis is applied. The Michigan State University works [10,17] claimed possible feeding-back of about 25%, based on their observation of another γ line at 1436 keV [17], which is supposed to feed the 2_1^+ state, resulting in $B(E2)$ values of $330(70)\ e^2\,\mathrm{fm}^4$ [17] and $328(48)\ e^2\,\mathrm{fm}^4$ [10]. These values are considerably smaller than the previously mentioned results and the present results. A significantly larger value of $622(90)\ e^2\,\mathrm{fm}^4$ was obtained by an experiment at the Grand Accelerateur National d'Ions Lourds (GANIL) [18]. Because a similar amount of feeding correction was applied in this work, the discrepency should originate from the experimental data.

IV. SUMMARY

The Coulomb excitation of ^{32}Mg at 195 MeV/nucleon was studied with a thick ($3.37\mathrm{g/cm}^2$) lead target. The angular scattering distribution for the 2^+ state excitation was obtained using in-beam γ-ray spectroscopy in coincidence with outgoing ^{32}Mg particles. By correcting for the γ-ray feeding from higher-lying states, the $B(E2\uparrow)$ value was extracted to be $432(51)\ e^2\,\mathrm{fm}^4$. The effect of nuclear excitation was evaluated based on a separate experiment of proton inelastic scattering taking into account the sensitivity depending on the probe particle and the incident energy. The present results agree with most of the earlier results within the errors, providing a sound demonstration for the usefulness of the Coulomb excitation method for extracting $B(E2)$ values at high incident energies around 200 MeV/nucleon. A target several times thicker than that usually used at lower energies is applicable when the effect of nuclear interaction is carefully incorporated by analyzing the angular distribution. It should be noted that the contribution from nuclear excitation is stronger for lighter nuclei and at higher energies. Coulomb excitation at this energy regime with thick targets opens new research opportunities to access nuclei very far from the β-stability line, where RI beams with significantly high intensities, produced from the new generation of projectile-fragmentation facilities, are now becoming available.

ACKNOWLEDGMENTS

We thank the RIKEN Nishina Center accelerator staff for the excellent facility operation during the experiment. One of the authors (K.L.) is grateful for the IPA program at RIKEN. K.L. also thanks the Institute of Modern Physics, CAS, for support in the preparation of the manuscript. This work is partly supported by the 973 project of China (Grant No. 2013CB834402) and the National Natural Science Foundation of China (Grants No. 11035001 and No. 11275011).

[1] K. Alder *et al.*, Rev. Mod. Phys. **28**, 432 (1956).
[2] P. H. Stelson and F. K. McGowan, Annu. Rev. Nucl. Sci. **13**, 163 (1963).
[3] K. Alder and A. Winter, *Electromagnetic Excitation* (North-Holland, Amsterdam, 1975).
[4] T. Motobayashi *et al.*, Phys. Lett. B **346**, 9 (1995).
[5] T. Glasmacher, Annu. Rev. Nucl. Part. Sci. **48**, 1 (1998).
[6] A. Gade *et al.*, Phys. Rev. C **68**, 014302 (2003).
[7] M. Fauerbach *et al.*, Phys. Rev. C **56**, R1 (1997).
[8] K. L. Yurkewicz *et al.*, Phys. Rev. C **70**, 034301 (2004).
[9] H. Scheit *et al.*, Phys. Rev. Lett. **77**, 3967 (1996).
[10] J. A. Church *et al.*, Phys. Rev. C **72**, 054320 (2005).
[11] A. Banu *et al.*, Phys. Rev. C **72**, 061305(R) (2005).
[12] A. Burger *et al.*, Phys. Lett. B **622**, 29 (2005).
[13] G. Guastalla *et al.*, Phys. Rev. Lett. **110**, 172501 (2013).
[14] P. Doornenbal *et al.*, Phys. Rev. C **90**, 061302 (2014).
[15] E. K. Warburton, J. A. Becker, and B. A. Brown, Phys. Rev. C **41**, 1147 (1990).
[16] H. Iwasaki *et al.*, Phys. Lett. B **522**, 227 (2001).
[17] B. V. Pritychenko *et al.*, Phys. Lett. B **461**, 322 (1999).
[18] V. Chiste *et al.*, Phys. Lett. B **514**, 233 (2001).
[19] T. Kubo *et al.*, IEEE Trans. Appl. Supercond. **17**, 1069 (2007).
[20] T. Ohnishi *et al.*, J. Phys. Soc. Jpn. **77**, 083201 (2008).
[21] T. Kubo *et al.*, Prog. Theor. Exp. Phys. **2012**, 03C003 (2012).
[22] Y. Yano, Nucl. Instrum. Methods Phys. Res., Sect. B **261**, 1009 (2007).
[23] H. Okuno, N. Fukunishi, and O. Kamigaito, Prog. Theor. Exp. Phys. **2012**, 03C002 (2012).
[24] H. Kumagai *et al.*, Nucl. Instrum. Methods Phys. Res., Sect. A **470**, 562 (2001).
[25] S. Takeuchi *et al.*, Nucl. Instrum. Methods Phys. Res., Sect. A **763**, 596 (2014).
[26] S. Agostinelli *et al.*, Nucl. Instrum. Methods Phys. Res., Sect. A **506**, 250 (2003).
[27] Y. Mizoi *et al.*, RIKEN Accel. Prog. Rep. **38**, 297 (2005).
[28] J. Raynal, coupled-channel code ECIS97 (unpublished).
[29] S. Takeuchi *et al.*, Phys. Rev. C **79**, 054319 (2009).
[30] T. Furumoto, W. Horiuchi, M. Takashina, Y. Yamamoto, and Y. Sakuragi, Phys. Rev. C **85**, 044607 (2012).
[31] K. Li *et al.*, Chinese Phys. Lett. **29**, 102301 (2012).
[32] Z. Elekes, N. Aoi, Zs. Dombrádi, Zs. Fülöp, T. Motobayashi, and H. Sakurai, Phys. Rev. C **78**, 027301 (2008).
[33] T. Motobayashi, Nucl. Phys. A **693**, 258 (2001).